

Expanded View Figures

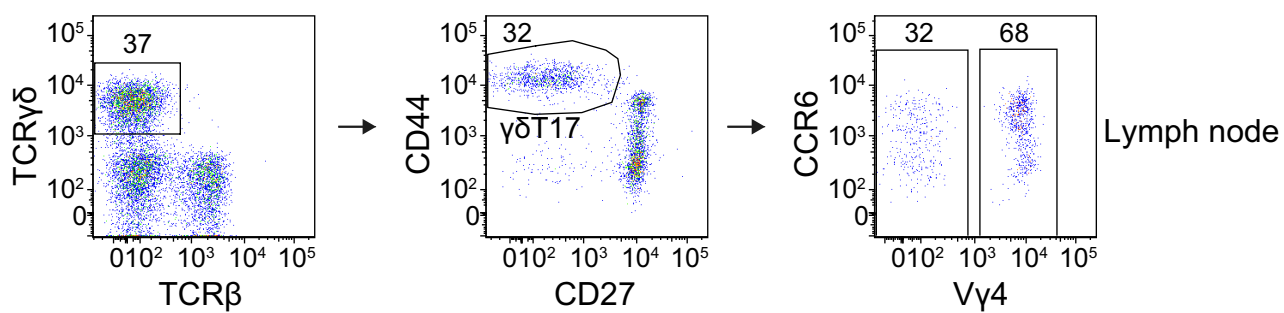
Figure EV1. Gating strategy for the identification of $\gamma\delta$ T17 cells by flow cytometry in lymph nodes and ear skin and assessment of the ROR γ t^{CRE} efficiency.

Flow cytometric analysis of $\gamma\delta$ T cells to indicate the gating strategy used to identify $\gamma\delta$ T17 cells in lymph node and skin and to assess the efficiency of the ROR γ t^{CRE}. In graph, each symbol represents a mouse and line the median.

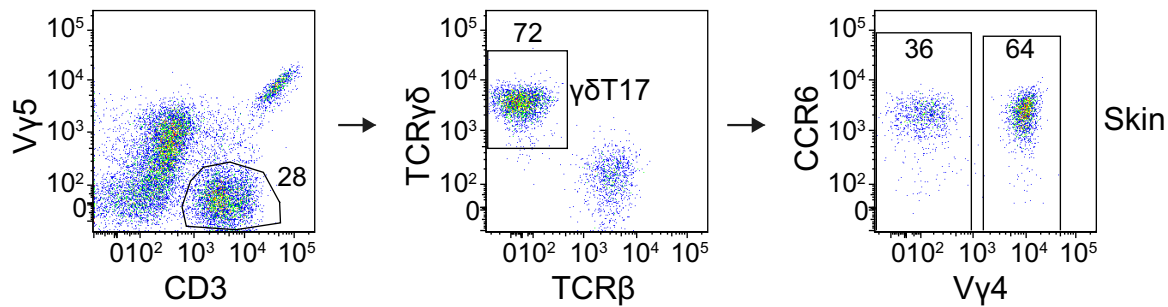
A, B Gating strategy in the lymph node (A) and skin (B).

C ROR γ t^{CRE} mice were crossed with ROSA26-STOPflox-RFP mice (ROR γ t^{CRE}-RFP^{STOP-F/F}), whereby the floxed STOP cassette in front of the red fluorescent protein (RFP) gene prevents its constitutive driven expression by the ROSA26 locus until Cre recombinase-mediated excision. The graph summarizes data from 4 mice. Each color represents a cell population.

Data information: In all FACS plots, numbers in gates indicate % of positive cells.

A

Lymph node

B

Skin

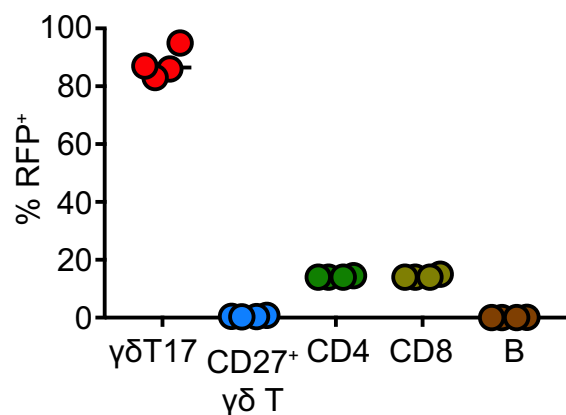
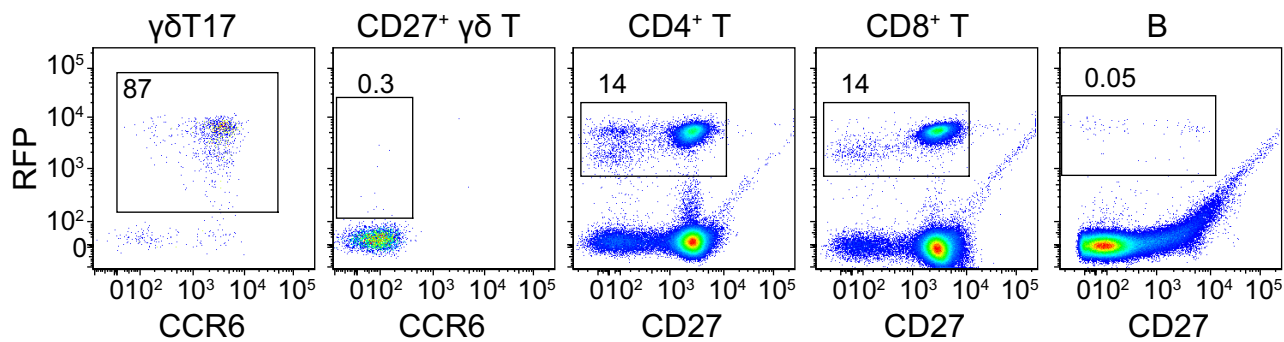
C

Figure EV1.

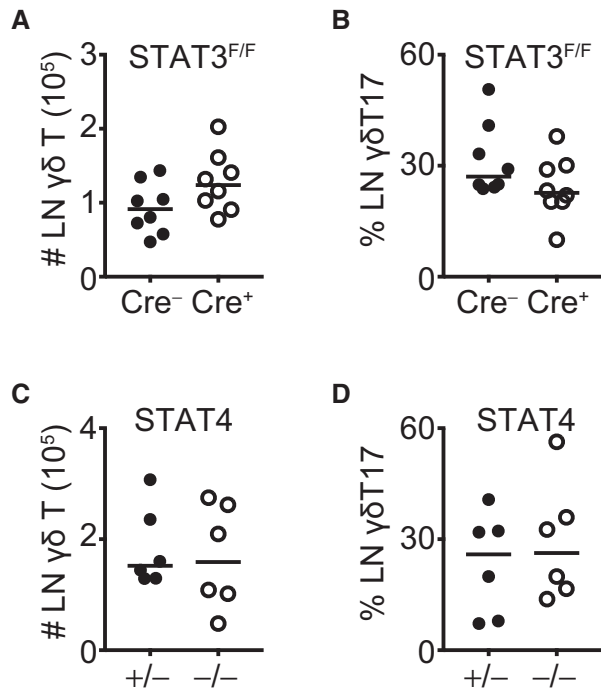


Figure EV2. STAT3 and STAT4 do not regulate $\gamma\delta$ T and $\gamma\delta$ T17 cell numbers in the lymph nodes.

Flow cytometric analysis of $\gamma\delta$ T cells in $ROR\gamma t^{CRE-STAT3^{F/F}}$ (Cre^+) and littermate control mice (Cre^-) (A-B) or in $STAT4^{-/-}$ ($-/-$) and littermate control mice ($+/-$) (C-D). In graphs, each symbol represents a mouse and line the median.

- A Numbers of total $\gamma\delta$ T cells in the LN of $ROR\gamma t^{CRE-STAT3^{F/F}}$ mice.
- B Frequency of $\gamma\delta$ T17 cells (% of total $\gamma\delta$ T) in the LN of $ROR\gamma t^{CRE-STAT3^{F/F}}$ mice.
- C Numbers of total $\gamma\delta$ T cells in the LN of $STAT4^{-/-}$ mice.
- D Frequency of $\gamma\delta$ T17 cells (% of total $\gamma\delta$ T) in the LN of $STAT4^{-/-}$ mice.

Data information: In (A-B), $n = 8$; 4 experiments. In (C, D), $n = 6$; 3 experiments.

Figure EV3. Impact of STAT3 and STAT4 on V γ 4 $^+$ and V γ 4 $^-$ $\gamma\delta$ T17 subsets in the lymph node and skin at steady state and during inflammation.

Flow cytometric analysis of $\gamma\delta$ T cells in $ROR\gamma t^{CRE-STAT3^{F/F}}$ (Cre^+) and littermate control mice (Cre^-) (A-D) or in $STAT4^{-/-}$ ($-/-$) and littermate control mice ($+/-$) (E-H). In graphs, each symbol represents a mouse and line the median. * $P < 0.05$, ** $P < 0.01$, *** $P < 0.001$ using Mann-Whitney test.

A-H (A, B and E, F) Numbers of V γ 4 $^+$ (A and E) and V γ 4 $^-$ (B and F) $\gamma\delta$ T17 cells in the LN before (steady state) and after IMQ-induced psoriasis in $ROR\gamma t^{CRE-STAT3^{F/F}}$ (A, B) or $STAT4^{-/-}$ (E, F) mice. Steady state: $n = 7-8$; 4 experiments, IMQ: $n = 11-12$; 4 experiments. (C, D and G, H) Numbers of V γ 4 $^+$ (C and G) and V γ 4 $^-$ (D and H) $\gamma\delta$ T17 cells in the skin before (steady state) and after IMQ-induced psoriasis in $ROR\gamma t^{CRE-STAT3^{F/F}}$ (C, D) or $STAT4^{-/-}$ (G, H) mice. Steady state: $n = 7-8$; 4 experiments, IMQ: $n = 11-12$; 4 experiments.

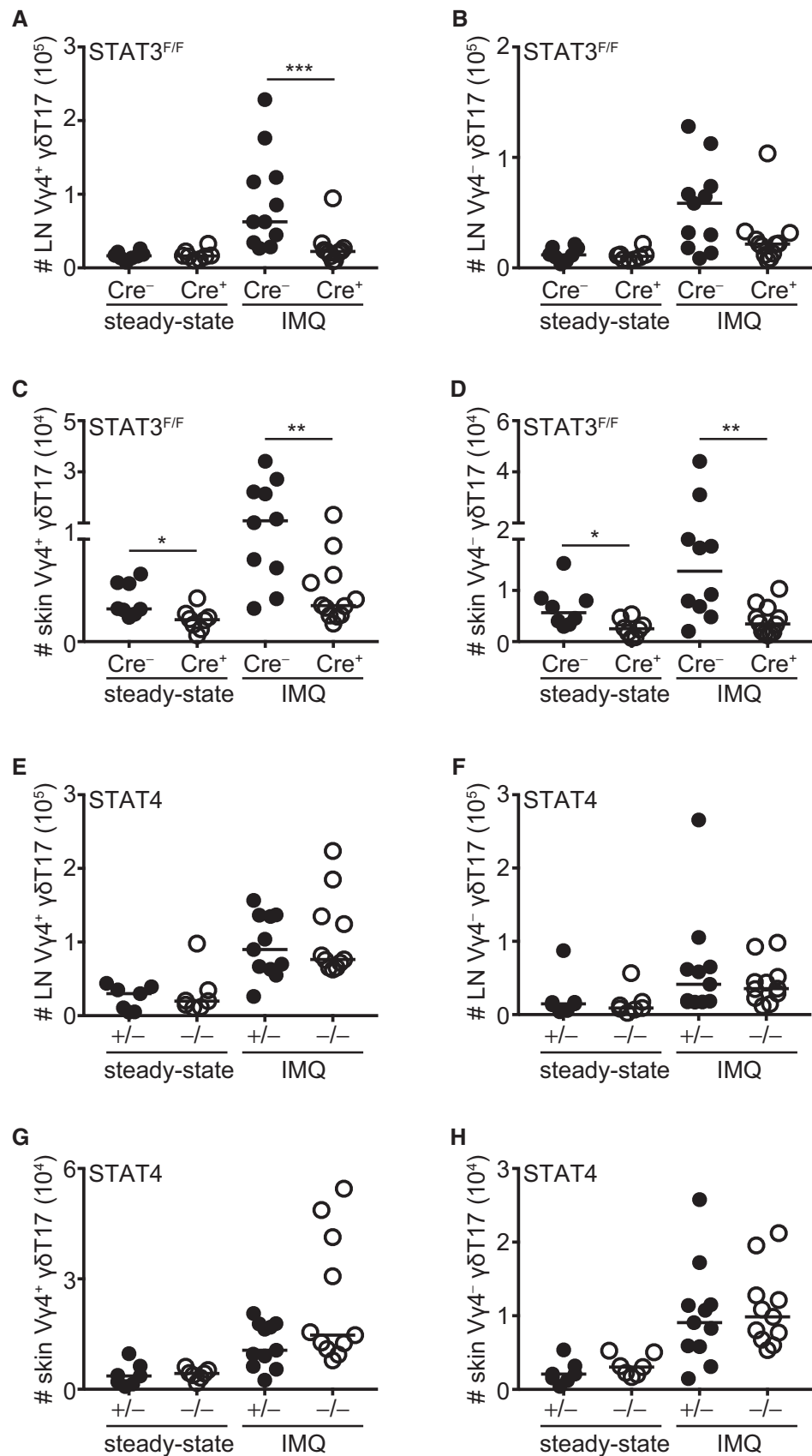


Figure EV3.

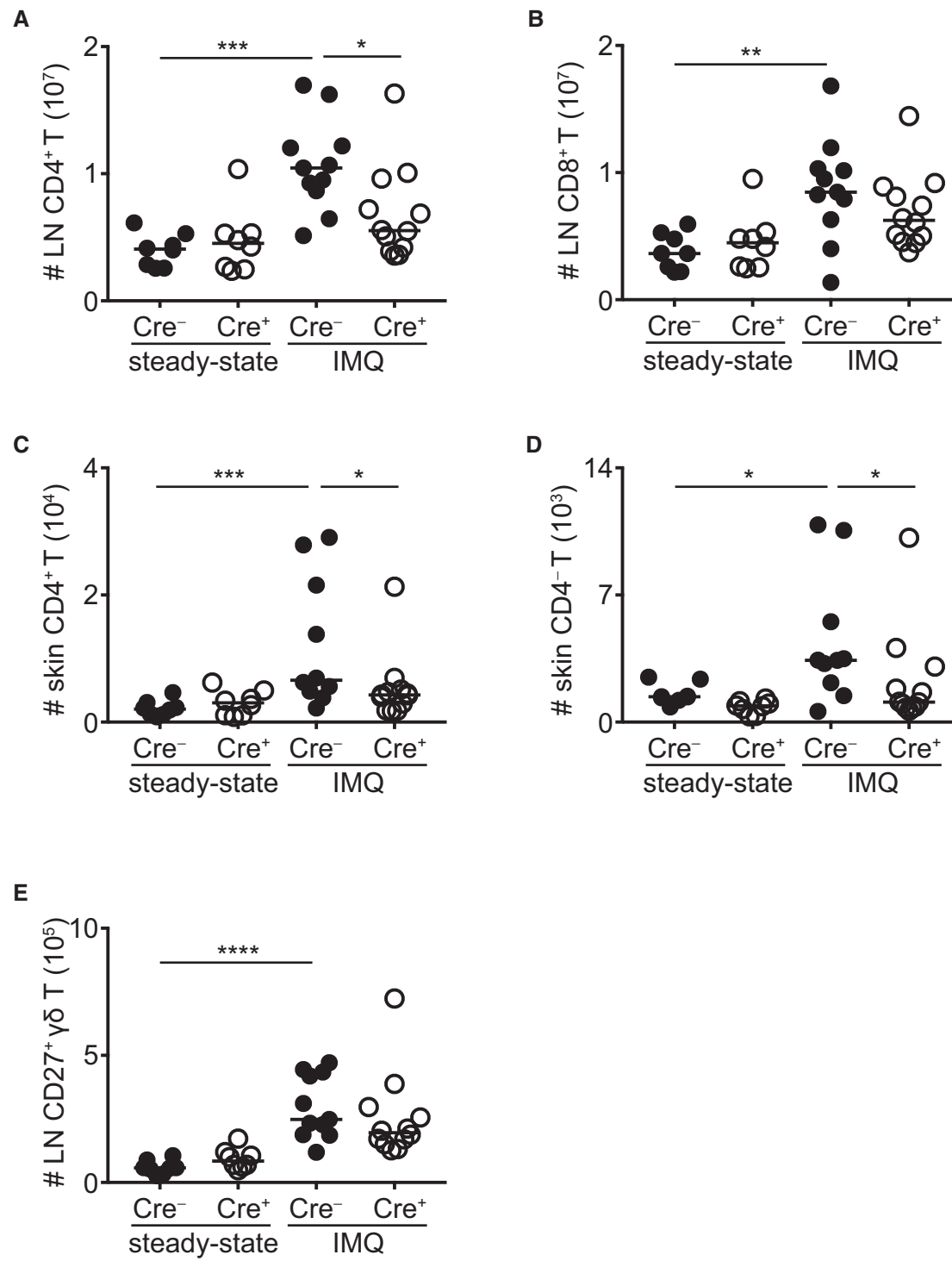


Figure EV4. Impact of STAT3 on non- $\gamma\delta$ T17 cell populations.

Flow cytometric analysis of lymph node or skin lymphocytes in ROR γ T^{CRE-STAT3^{F/F} (Cre $^+$) and littermate control mice (Cre $^-$). In graphs, each symbol represents a mouse and line the median. *P < 0.05, **P < 0.01, ***P < 0.001, ****P < 0.0001 using Mann-Whitney test.}

A, B Numbers of LN CD4⁺ and CD8⁺ T cells before (steady state) and after IMO treatment.

C, D Numbers of skin CD4⁺ and CD4⁻ T cells before (steady state) and after IMO treatment.

E Numbers of LN CD27⁺ $\gamma\delta$ T cells before (steady state) and after IMO treatment.

Data information: Steady state: $n = 8$; 4 experiments, IMO; $n = 11-12$; 4 experiments

Figure EV5. Contribution of $\gamma\delta$ and $\alpha\beta$ T cells toward production of IL-17A, IL-17F, and IL-22 during IMQ-induced inflammation.

Flow cytometric analysis of IL-17A-, IL-17F-, and IL-22-producing T cells in the lymph node during IMQ-induced inflammation. In graphs, each symbol represents a mouse and line the median. *** $P < 0.001$, **** $P < 0.0001$ using Mann–Whitney test.

A, B Frequency of IL-17A $^+$ (A) or IL-17F $^+$ (B) cells that are either TCR $\gamma\delta^+$ or TCR β^+ within the total IL-17A- or IL-17F-producing population.

C Frequency of IL-22 $^+$ cells that are either TCR $\gamma\delta^+$ or TCR β^+ within the total IL-17A-producing population.

D Frequency of CD4 $^+$ and CD4 $^-$ IL-22 $^+$ T cells in ROR γ t $^{CRE-STAT3^{FL}}$ (Cre $^+$) and littermate control mice (Cre $^-$) at steady state or after IMQ treatment.

Data information: (A–D) $n = 8–11$; 3–4 experiments. In FACS plots, numbers in gate indicate % positive cells.

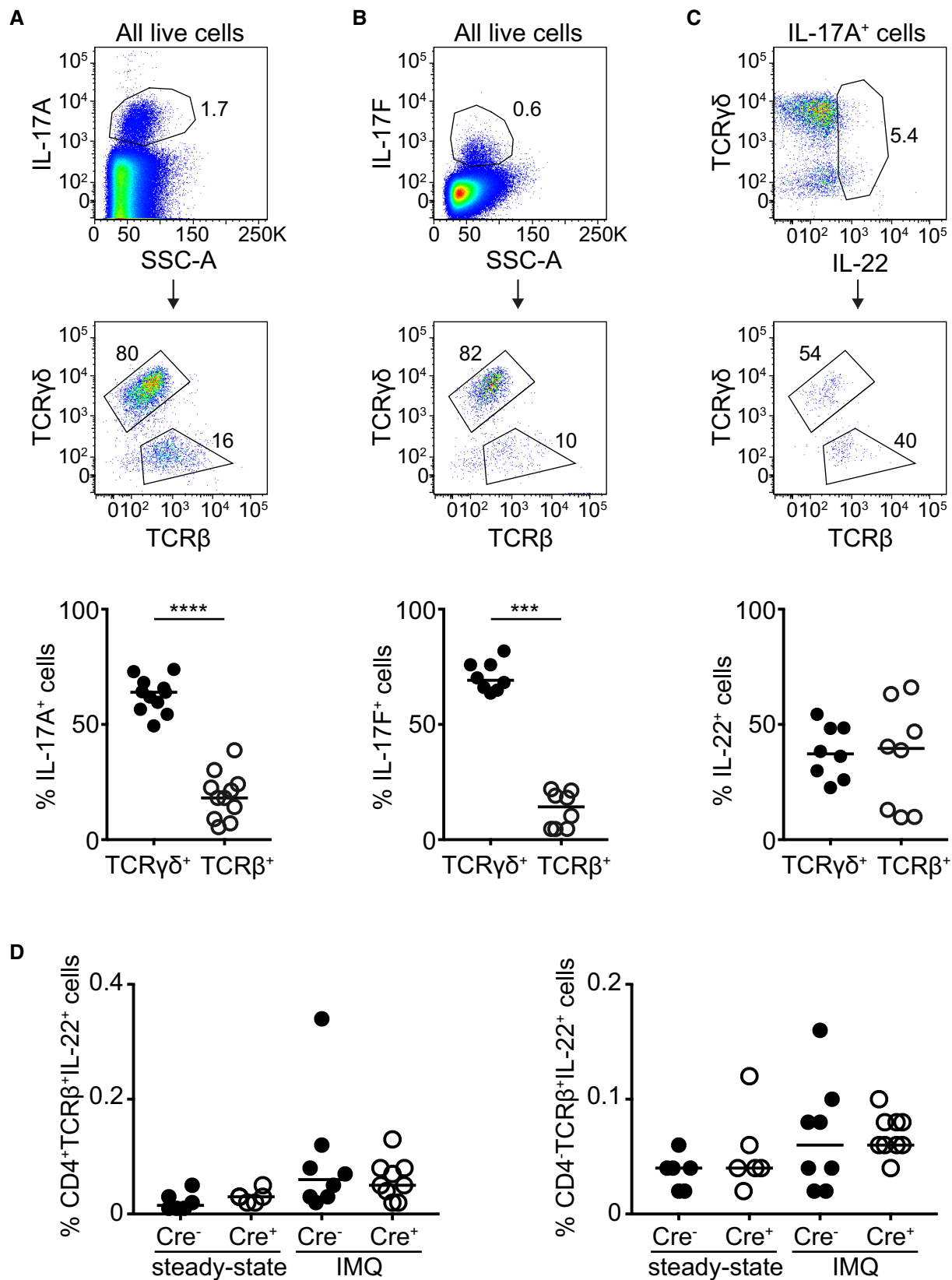


Figure EV5.